Available online at www.sciencedirect.com
SCIENCE DIRECT®
Nuclear Instruments and Methods in Physics Research B 247 (2006) 210–216
NIM B
Beam Interactions with Materials & Atoms
www.elsevier.com/locate/nimb

Cross sections of deuteron induced nuclear reactions on iridium

F. Tárkányi [a,*], B. Király [a], F. Ditrói [a], S. Takács [a], J. Csikai [a,e], A. Hermanne [b], M.S. Uddin [c], M. Hagiwara [c], M. Baba [c], Yu.N. Shubin [d], S.F. Kovalev [d]

[a] Institute of Nuclear Research of the Hungarian Academy of Sciences (ATOMKI), Cyclotron Department, Bem ter 18c, 4026 Debrecen, Hungary
[b] Cyclotron Laboratory, Vrije Universiteit Brussel, 1090 Brussels, Belgium
[c] Cyclotron and Radioisotope Center, Tohoku University, Sendai 980-8578, Japan
[d] Institute of Physics and Power Engineering, Obninsk 249020, Russian Federation
[e] Institute of Experimental Physics, University of Debrecen, 4026 Debrecen, Hungary

Received 9 November 2005; received in revised form 13 February 2006
Available online 18 April 2006

Abstract

Excitation functions of the reactions $^{nat}Ir(d,xn)^{188,189,191,193m}Pt$ and $^{nat}Ir(d,x)^{189,190g,192g,194g,194m2}Ir$ were measured up to 40 MeV using the stacked foil technique. No earlier cross sections were found in the literature. The measured experimental data were analyzed and compared to theoretical calculations based on the model code ALICE-IPPE. Use of the experimental cross sections for practical applications is also discussed.

PACS: 25.45.−z; 27.70.+q; 27.80.+w

Keywords: Iridium target; Excitation function; Deuteron irradiation; Cyclotron; Platinum and iridium radioisotopes

1. Introduction

This work was performed in the frame of a systematic study of excitation functions of light charged particle induced nuclear reactions on metal targets in the medium energy range. We are preparing a recommended database for thin layer activation technique (TLA) that includes all candidate reactions on metals [1]. In this project activation cross sections on iridium are important because its possible presence can induce interferences during nuclear data measurements in noble metal targets. Furthermore, we are investigating excitation functions of longer lived products of light charged particle induced nuclear reactions on metals to estimate activation dose rates for accelerator and target technology.

It is also well known that different Pt or Ir radioisotopes (^{191}Pt, ^{193}Pt and ^{192}Ir, ^{194}Ir) are relevant in medical practice (tumor chemotherapy, brachytherapy, radioimmunotherapy, radioactive source in dual-energy computerized tomography) and as radiotracers for environmental and biological studies as well as in automotive catalytic converters. The favorite production routes of these radioisotopes are neutron induced reactions on enriched Ir or Pt targets. However, for laboratories having access to accelerators, it can be important to investigate alternative methods using charged particle reactions on Os, Ir, Pt and Au.

So, we decided to study the excitation functions of deuteron induced reactions on iridium using proton-, deuteron- and alpha-beams.

No earlier experimental results were found in the literature for deuteron induced reactions. Our results on proton induced reactions were reported in [2]. Some preliminary results on deuteron induced reactions on ^{nat}Ir were presented at the 5th International Conference on Isotopes, Brussels, Belgium, 2005 [3].

* Corresponding author. Tel.: +36 52 509200; fax: +36 52 416181.
E-mail addresses: tarkanyi@atomki.hu (F. Tárkányi), kiralyb@atomki.hu (B. Király).

0168-583X/$ - see front matter © 2006 Elsevier B.V. All rights reserved.
doi:10.1016/j.nimb.2006.03.002

2. Experimental procedures

The standard stacked foil irradiation method was used to measure the cross sections. Two irradiations were carried out with low intensity external beams of the cyclotrons at the Tohoku University, Japan (we refer to it as stack1) and at the Vrije Universiteit Brussel, Belgium (stack2). The irradiations were done with initial deuteron energy of 40 and 21 MeV, for 27 and 23 min, using 128 and 120 nA beam currents, respectively. The target stack was formed of ^{nat}Ir foils, interlarded with Al (stack1) and Ti monitor foils (stack2) to control the beam parameters. The beam intensity and the energy degradation along the stack were controlled via the monitor reactions ^{27}Al(d, x)^{22,24}Na and ^{nat}Ti(d, x)^{48}V using the recommended values of [4,5] (see Fig. 1).

The gamma spectra of the irradiated iridium and monitor foils were measured without chemical separation using high purity germanium detectors. The absolute overall detection efficiency (intrinsic and geometric effects are coupled) in the photopeaks was calibrated at several source–detector distances using certified point-like energy standards. Large source–detector distances for measurement of the activated foils were used to minimize the detector dead time, pile-up effects and coincidence losses and to minimize possible geometrical effects caused by the extended dimensions (several millimeters) of the samples.

The counting was started about 20 (stack1) and 2 (stack2) h after the EOB (end of bombardment). Three series of measurements were done in both cases which continued for several weeks. This procedure allows following the build up of cumulative effects and helps in the decomposition of gamma lines originating from different isotopes. As the gamma spectra were very complex an interactive spectrum analysis procedure available in the FGM analyzing software developed in Dubna [6] and iterative data evaluation (corrections for contribution of contaminating signals) were used for proper separation and identification of the different activation products.

Independent and cumulative elemental cross sections were calculated supposing the target to be monoisotopic.

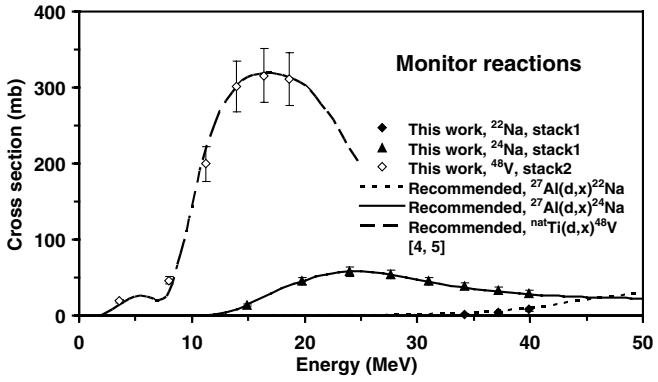

Fig. 1. Excitation functions of the ^{27}Al(d, x)^{22,24}Na and ^{nat}Ti(d, x)^{48}V monitor reactions.

Natural iridium includes two stable isotopes: ^{191}Ir and ^{193}Ir with abundance of 37.3% and 62.7%, respectively. The decay data of the investigated reaction products are summarized in Table 1 [7]. The median deuteron energy in the successive target foils was determined from the bombarding energy, stack composition and foil thickness by calculation [8] and, if needed, was corrected on the basis of the simultaneously remeasured excitation function of the monitor reactions.

The uncertainties were estimated in the standard way [9]; the linearly contributing independent processes were taken into account extracting square root of quadratically summed relative uncertainties, namely: number of the bombarding particles (7%), number of the target nuclei (3%), decay data (3%), detector efficiency (5%) and peak area (1–10%). The uncertainty of the energy of the bombarding beam in the middle of each irradiated foil was estimated combining the uncertainties of the energy degradation depending on the thickness of the target foils in the stack and the energy straggling.

More details on the irradiation technique and the data evaluation can be found in earlier reports [10,11]. Regarding the decay schemes we refer to our work on activation cross sections of proton induced nuclear reactions on ^{nat}Ir [2].

Table 1
Decay characteristics of the investigated reaction products [7]

Nuclide	Half-life	E_γ (keV)	I_γ (%)
^{188}Pt	10.2 d	195.05	18.6
		381.43	7.5
		423.34	4.36
^{189}Pt	10.87 h	243.37	7.0
		721.41	9.3
^{191}Pt	2.80 d	172.18	3.52
		351.21	3.36
		359.90	6.0
		409.44	8.10
		456.5	3.36
^{193m}Pt	4.33 d	135.50	0.11
^{189}Ir	13.2 d	245.09	6
^{190g}Ir	11.78 d	371.26	23
		407.24[a]	28.5[b]
		518.55	34.0
		557.97	30.1
		569.31	28.5
^{192g}Ir	73.83 d	295.96	28.67
		308.46	30.00
		316.51	82.81
		468.07	47.83
^{194g}Ir	19.28 h	293.55	2.52
		328.46	13.1
^{194m2}Ir	171 d	338.8	55
		482.83	97
		562.6[c]	70[d]
		687.7	59

[a] From two lines: (407.176 keV·23.9% + 407.543 keV·4.6%)/(23.9% + 4.6%).
[b] 23.9% + 4.6%.
[c] From two lines: (562.5 keV·35% + 562.64 keV·35%)/(35% + 35%).
[d] 35% + 35%.

3. Model calculation

The measured experimental data were compared and analyzed with theoretical calculations based on the model code ALICE-IPPE. The ALICE code family was developed by Blann [12] and is based on the hybrid, the geometry-dependent hybrid (GDH) or the hybrid Monte Carlo simulation (HMS) pre-equilibrium models and the Weisskopf–Ewing evaporation formalism. The ALICE-IPPE code [13] is a version of the ALICE-91 code [14] modified by the Obninsk Group to include the generalized superfluid level density model and pre-equilibrium cluster emission. Corrections were made, among others, for gamma-emission and optical model parameters. Angular distribution and refraction were not taken into account.

The lack of angular momentum and parity treatments in the Weisskopf–Ewing formalism used makes independent treatment of isomeric states impossible, only total production cross sections can be calculated. The individual results of the reaction products of interest in this study were weighted and summed according to the abundance of the target isotopes and to the cumulative processes. Direct comparison of the experimental results with a-priori model calculations (one recommended input data-set without any optimization or adjustment of parameters to the individual reactions or stable target isotopes) that in general represent well the presence of different reaction channels for a given end product, allows having an increased confidence in experimental data if a similar energy dependent shape is found for complex excitation functions.

4. Results

4.1. Cross sections

Cross sections of the nuclear reactions ^{nat}Ir(d, xn)^{188,189,191,193m}Pt and ^{nat}Ir(d, x)^{189,190g,192g,194g,194m2}Ir were determined and compared to the results of model calculation. In Figs. 2–9 we present the measured cross sections and the results of the model calculation. The numerical values of the cross sections are collected in Tables 2 and 3. The different reaction products are discussed below.

Note that in this work cumulative means the cross section which includes the cross sections of parent nuclei and/or isomer states after their total decay in addition to the referred nucleus so cumulative cross sections are valid only after the proper cooling time. Moreover note that in this work expressions like direct reaction, direct process etc. do not refer to the reaction mechanism but mean that there is no decay into the referred nucleus and are used to enhance that no cumulative process takes place.

4.1.1. $^{nat}Ir(d, xn)^{188}Pt$ process

In the investigated energy range only the ^{191}Ir(d, 5n) reaction contributes to the production of ^{188}Pt. The excitation function is shown in Fig. 2. The agreement between the experiment and the theory is good.

4.1.2. $^{nat}Ir(d, xn)^{189}Pt$ process

There is a good agreement between the data measured experimentally and calculated with the ALICE-IPPE code (see Fig. 3). Up to 40 MeV only the ^{191}Ir(d, 4n) reaction contributes to the production.

4.1.3. $^{nat}Ir(d, xn)^{191}Pt$ process

According to Fig. 4 our experimental values are systematically 30–40% lower than the theoretical prediction. The first peak of the excitation function is due to the ^{191}Ir(d, 2n) reaction and the other one is due to the ^{193}Ir(d, 4n) reaction.

4.1.4. $^{nat}Ir(d, xn)^{193m}Pt$ process

The product nucleus does not emit gammas after the ground state is populated and it emits very poor and low-energy gammas when the metastable state decays (see Table 1). It was possible to measure this weak gamma line

Table 2
Measured cross sections of the reactions ^{nat}Ir(d, xn)^{188,189,191,193m}Pt

Deuteron		^{188}Pt		^{189}Pt		^{191}Pt		^{193m}Pt	
Energy (MeV)	ΔE (MeV)	σ (mb)	$\Delta\sigma$ (mb)	σ (mb)	$\Delta\sigma$ (mb)	σ (mb)	$\Delta\sigma$ (mb)	σ (mb)	$\Delta\sigma$ (mb)
1.7	1.5								
5.8	1.1					3.1	0.4	9.0	4.7
6.8	1.8					6.0	3.7		
9.6	0.8					73.1	8.7	65	15
12.6	0.7					172	21	233	59
13.1	1.6	0.71	0.37			155	22		
15.2	0.5					159	19	137	37
16.5	1.4	0.51	0.21			129	21		
17.5	0.5					108	13	82	27
19.7	0.3					74.4	9.5	69	19
21.1	1.2			1.1	0.5	80	16		
25.1	1.0			93	11	301	40		
28.7	0.8			261	30	510	70		
32.0	0.6	8.8	4.7	335	39	529	73		
35.1	0.4	64	15	341	40	456	64		
38.0	0.3	156	22	264	30	309	37		

Table 3
Measured cross sections of the reactions $^{nat}Ir(d,x)^{189,190g,192g,194g,194m2}Ir$

Deuteron		Cum ^{189}Ir		Cum ^{190g}Ir		Cum ^{192g}Ir		^{194g}Ir		$^{194m2}Ir$	
Energy (MeV)	ΔE (MeV)	σ (mb)	$\Delta\sigma$ (mb)	σ (mb)	$\Delta\sigma$ (mb)	σ (mb)	$\Delta\sigma$ (mb)	σ (mb)	$\Delta\sigma$ (mb)	σ (mb)	$\Delta\sigma$ (mb)
1.7	1.5			0.09	0.02	0.51	0.23	0.25	0.13	0.36	0.10
5.8	1.1			0.09	0.08	9.1	1.3	16.0	1.8	0.11	0.10
6.8	1.8	0.58	0.13	1.9	0.2	15.2	2.2	22.5	3.8		
9.6	0.8			1.6	0.2	65.3	7.9	110	13	0.24	0.15
12.6	0.7			7.5	1.0	97	12	141	16	0.38	0.37
13.1	1.6			8.5	1.0	96	12	126	18	0.22	0.06
15.2	0.5			11.6	1.4	95	11	124	15	0.44	0.31
16.5	1.4			13.1	1.5	92	11	103	12	0.44	0.09
17.5	0.5			13.2	1.9	88	12	104	12	0.61	0.29
19.7	0.3			15.6	1.9	81	10	88	10	0.27	0.22
21.1	1.2	13.7	2.3	17.4	2.0	80.1	9.7	71.1	8.4	0.44	0.09
25.1	1.0	92	10	34.7	4.1	105	14	54.7	7.2	0.36	0.09
28.7	0.8	263	30	59.3	6.9	141	19	44.8	7.4	0.42	0.12
32.0	0.6	341	38	78.2	9.1	158	19	39.4	6.8	0.31	0.12
35.1	0.4	351	39	94	11	185	25	31.6	4.4	0.71	0.21
38.0	0.3	248	28	98	11	176	23	25.3	5.9		

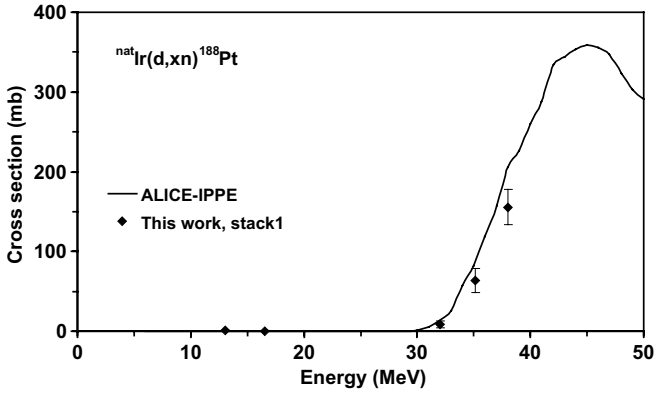

Fig. 2. Excitation function of the $^{nat}Ir(d,xn)^{188}Pt$ reaction.

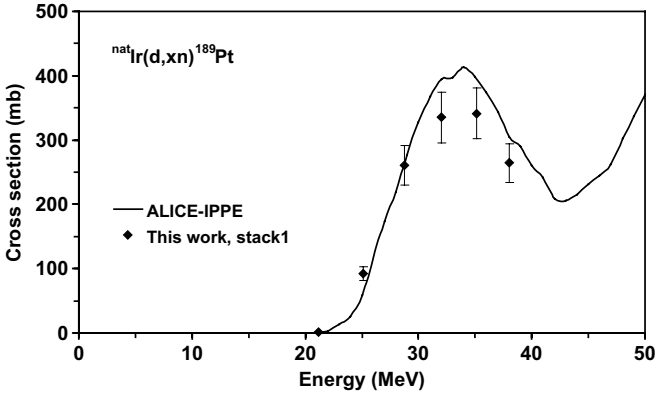

Fig. 3. Excitation function of the $^{nat}Ir(d,xn)^{189}Pt$ reaction.

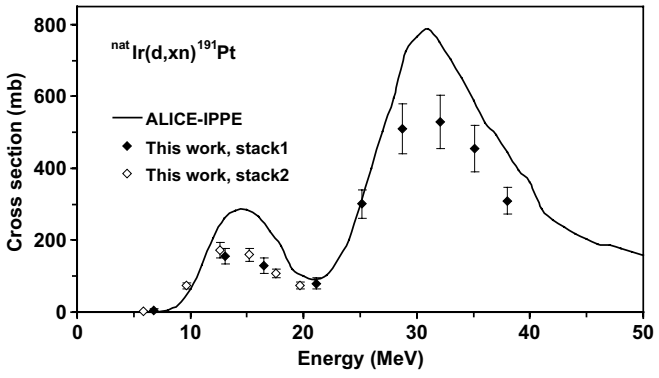

Fig. 4. Excitation function of the $^{nat}Ir(d,xn)^{191}Pt$ reaction.

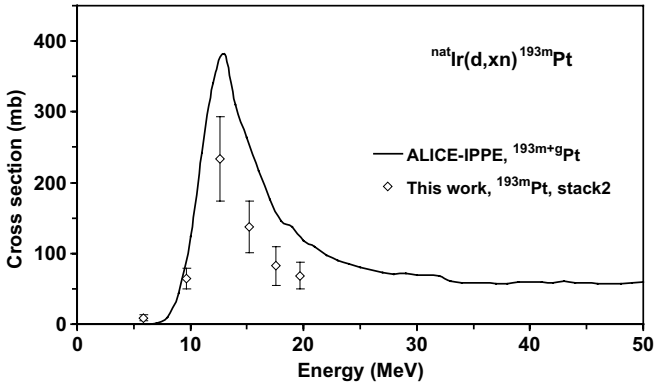

Fig. 5. Excitation function of the $^{nat}Ir(d,xn)^{193m}Pt$ reaction.

and to calculate cross sections for ^{193m}Pt subtracting the contribution from the similarly weak gamma line of ^{192g}Ir (136.34 keV, 0.183%). The ALICE-IPPE code cannot separate the cross sections of the two isomer states but it can calculate them together. The results are shown in Fig. 5. The ^{193}Pt is formed by $^{191}Ir(d,\gamma)$ and $^{193}Ir(d,2n)$ reactions, however, only the latter should be taken into account because the first one has no considerable contribution. The theoretical curve follows the shape of our experimental data points.

4.1.5. Cumulative $^{nat}Ir(d,x)^{189}Ir$ process

The cumulative cross sections measured for production of ^{189}Ir contain the contribution from ^{189}Pt (half-life: 10.87 h) after its complete decay. The agreement between the experiment and the theory is acceptable. Comparing the experimental excitation function of ^{189}Pt (Fig. 3) to the cumulative cross sections of ^{189}Ir (Fig. 6) it can be concluded that in the investigated energy range the direct production of ^{189}Ir is small compared to the production through the decay of ^{189}Pt. This remark is supported also by theoretical results (see Fig. 6).

4.1.6. Cumulative $^{nat}Ir(d,pxn)^{190g}Ir$ process

Results are shown in Fig. 7. The product nucleus has two high laying isomer states in addition to the ground state, the cross sections of which are also included with the proper weight in this cumulative cross section but there is no contribution from ^{190}Pt which is an alpha-decaying nucleus. In cross sections calculated with the ALICE-IPPE all parts (^{190g}Ir, ^{190m1}Ir and ^{190m2}Ir) are equally weighted while in cumulative cross sections measured experimentally the coefficient of ^{190m2}Ir is almost negligible because this isomer prefers beta-decay rather than isomeric transition. There is significant disagreement between the results measured and calculated with the model code.

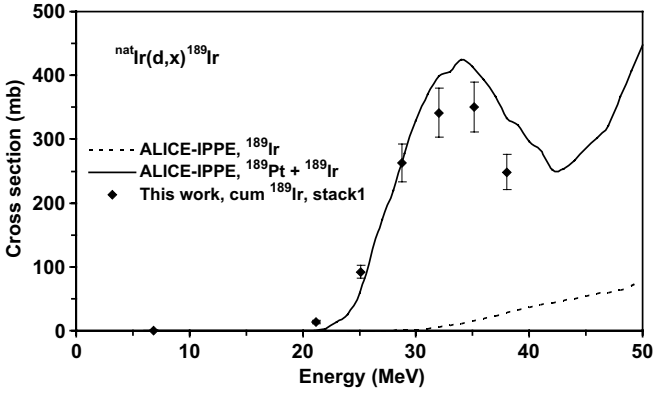

Fig. 6. Excitation function of the cumulative ^{nat}Ir(d, x)^{189}Ir reaction.

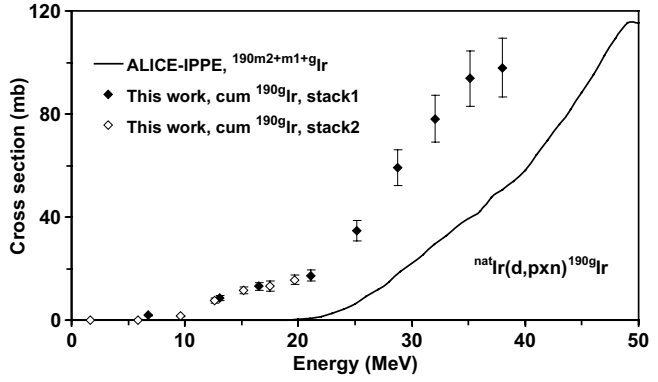

Fig. 7. Excitation function of the cumulative ^{nat}Ir(d, pxn)^{190g}Ir reaction.

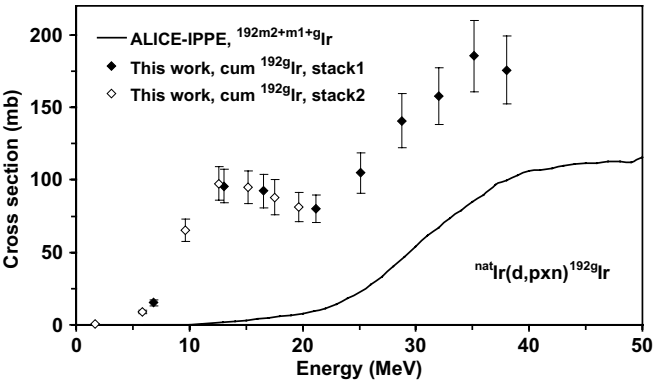

Fig. 8. Excitation function of the cumulative ^{nat}Ir(d, pxn)^{192g}Ir reaction.

4.1.7. Cumulative $^{nat}Ir(d,pxn)^{192g}Ir$ process

Results are shown in Fig. 8. The product nucleus has two metastable states; one of them (^{192m2}Ir) has a very long half-life (241 years) thus nearly zero counts originated from these nuclei during our measurement. The cumulative cross section hence consists of the cross sections of direct ^{192g}Ir formation and total decay of ^{192m1}Ir. The data calculated with the ALICE-IPPE code include the cross section of ^{192m2}Ir as well but significantly underestimate the measured data because (d, p) stripping is not well modeled.

4.1.8. $^{nat}Ir(d,pxn)^{194g}Ir$ and $^{nat}Ir(d,pxn)^{194m2}Ir$ processes

The product nuclei are produced only via the ^{193}Ir(d, p) reaction as ^{194}Os is not formed in this irradiation. The high spin (10, 11) metastable state does not decay into the low spin (1^-) ground state but prefers beta-decay. We determined excitation functions for production of both states separately. The ^{194m1}Ir has a very short half-life: 31.85 ms and decays into the ground state by IT so strictly speaking its cross section is also included in cross section of ^{194g}Ir. As it is shown in Fig. 9 the population of the ground state is significantly higher. The contradiction between the measured and predicted data can be explained by the fact that the model code cannot handle the stripping process.

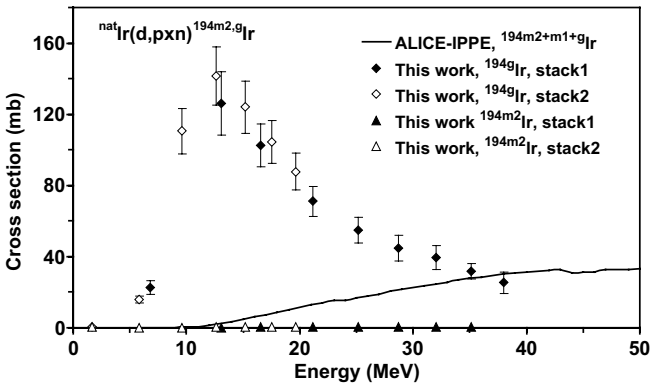

Fig. 9. Excitation functions of the ^{nat}Ir(d, pxn)^{194m2,g}Ir reactions.

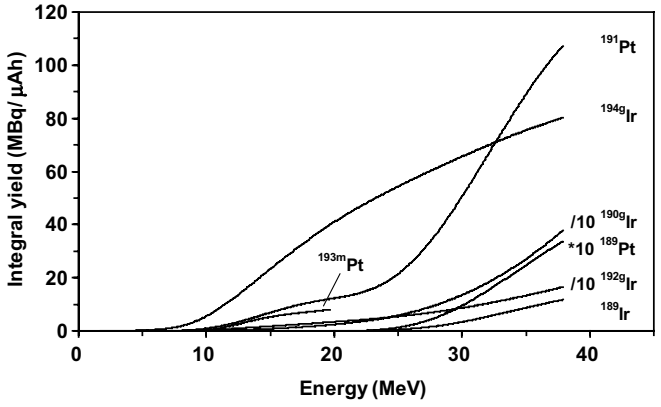

Fig. 10. Integral yields of $^{nat}Ir(d,x)^{189,191,193m}Pt$, $^{189,190g,192g,194g}Ir$ reactions. Values of ^{189}Pt must be multiplied and values of ^{190g}Ir and ^{192g}Ir must be divided by 10.

4.2. Integral yields

The physical yields for production of different Pt and Ir radioisotopes on pure metal Ir target were calculated from the excitation functions measured experimentally. The integral yields of $^{189,191,193m}Pt$ and $^{189,190g,192g,194g}Ir$ are shown in Fig. 10. No experimentally measured yields were found in the literature.

5. Applications

The knowledge of excitation functions of deuteron induced reactions on iridium is of direct importance in production of medically relevant radioisotopes (^{191}Pt, ^{193}Pt and ^{192}Ir). ^{191}Pt is used as a component of the radioactive cisplatin together with ^{193}Pt in tumor chemotherapy and as a radiotracer in environmental and biological samples as well as in automotive catalytic converters. The isotope ^{192}Ir is used as a radioactive source in the dual-energy computerized tomography, in brachytherapy for treatment of cancer disease and in the radiotracer technique for environmental and geological samples while ^{194}Ir is a suitable candidate for radioimmunotherapy. The favorite production routes of these radioisotopes are neutron induced reactions on enriched Ir or Pt targets. However, for laboratories having access to accelerators, it can be important to investigate alternative methods using charged particle reactions on Os, Ir, Pt and Au. Although the yields via the (n,γ) reactions in a reactor environment are mostly by several orders of magnitude higher than for charged particle reactions, the accelerator method has the advantage to lead to "no-carrier added" end products.

The isotope ^{191}Pt can be produced very effectively by the $^{191}Ir(d,2n)$ and $^{193}Ir(d,4n)$ processes (see Fig. 4). The optimal energy ranges for high production yield are 20–10 and 40–25 MeV, respectively. The yield will also be high using natural iridium. The disadvantage of the natural target is that simultaneously contaminants like ^{188}Pt and ^{189}Pt are produced at higher energies and ^{193}Pt also at lower energies. The amount of ^{189}Pt can be reduced by using an appropriate cooling time but this reduces the yield of ^{191}Pt. The long-lived product ^{188}Pt can be eliminated only by decreasing the energy of the bombarding beam below 30 MeV (Fig. 2). However, it does not help to eliminate the other long-lived isotope ^{193}Pt because the $^{193}Ir(d,2n)$ reaction disturbs practically at any energy ranges (Fig. 5). It can be concluded that using ^{nat}Ir target pure ^{191}Pt cannot be produced. However, limiting the incoming energy to 30 MeV a mixture of ^{191}Pt and ^{193}Pt can be produced which could be also effectively used in some applications. Using highly enriched ^{191}Ir target high purity ^{191}Pt can be produced below 20 MeV.

Production of high purity ^{193}Pt on ^{nat}Ir target is impossible due to the simultaneously produced ^{191}Pt (Fig. 4) (^{188}Pt and ^{189}Pt can be reduced as it was discussed above). Bombarding highly enriched ^{193}Ir with deuterons below 20 MeV, Pt radioisotopes are produced only via the $^{193}Ir(d,2n)^{193}Pt$ reaction because ^{192}Pt and ^{194}Pt are stable and the contributions of the reactions $^{193}Ir(d,\gamma)^{195m}Pt$ and $^{193}Ir(d,4n)^{191}Pt$ are negligible.

The production of ^{192}Ir via deuteron induced reaction on Ir target results in a carrier-added product. The cross section is not small due to the stripping process, but it cannot compete with neutron irradiations. Another drawback is that before use longer cooling time is needed to allow decaying the simultaneously produced ^{189}Ir and ^{190}Ir.

For accelerator technology, target activation and waste handling, integral yields of longer lived products were calculated from the excitation functions measured experimentally and are shown in Fig. 10.

The thin layer activation (TLA) method used for wear, erosion and corrosion studies requires reaction products with proper decay characteristics and high cross sections at low bombarding energies. None of the investigated reaction products can be produced effectively with a small cyclotron (10 MeV deuteron). For a 20 MeV cyclotron only the production of radionuclides ^{190}Ir and ^{192}Ir should be taken into account.

6. Summary

As it was mentioned the basic motivation of our measurements was to determine the possible contribution of iridium to radionuclide impurities in noble metal targets (palladium, rhodium, platinum, gold) since these targets are often used for production of medical radioisotopes. Our measured excitation functions can be effectively used to solve such problems.

Comparing the experimental data with the results of the model calculations acceptable agreements were found for (d,xn) reactions but in case of (d,pxn) reactions the ALICE-IPPE code cannot predict the excitation function due to the incorrect modeling of the stripping reactions (d,p) and (d,n). However, the model calculations are very useful because they can help in data evaluation, in understanding the contribution of different reactions to the

excitation function and in some ways they can validate the experimental results.

Acknowledgements

This work was performed in the frame of the projects HAS-JSPS (Hungary–Japan), HAS-FWO (Vlaanderen) (Hungary–Belgium) and OTKA (T037190). The authors acknowledge the support of the research project and of the respective institutions in providing the beam time and experimental facilities. One of the authors of this paper (F. Ditrói) is a grantee of the Bolyai János Scholarship of the Hungarian Academy of Sciences.

References

[1] F. Ditrói, S. Takács, F. Tárkányi, Evaluation of reaction cross section data used for thin layer activation technique, in: ND2004 Conference, Santa Fe, USA, 2004, Abstracts, p. 278.

[2] F. Tárkányi, B. Király, F. Ditrói, S. Takács, J. Csikai, A. Hermanne, M.S. Uddin, M. Hagiwara, M. Baba, T. Ido, Yu.N. Shubin, A.I. Dityuk, Activation cross sections of proton induced nuclear reactions on Iridium, Nucl. Instr. and Meth. B 239 (2005) 293.

[3] F. Tárkányi, B. Király, F. Ditrói, S. Takács, J. Csikai, A. Hermanne, M.S. Uddin, M. Hagiwara, M. Baba, Yu.N. Shubin, S.F. Kovalev, Activation cross sections of deuteron induced nuclear reactions on iridium, in: 5th International Conference on Isotopes (5ICI), Brussels, Belgium, 25–29 April 2005, Abstract Book, p. 52.

[4] F. Tárkányi, S. Takács, K. Gul, A. Hermanne, M.G. Mustafa, M. Nortier, P. Oblozinsky, S.M. Qaim, B. Scholten, Yu.N. Shubin, Z. Youxiang, Beam monitor reactions, in: Charged Particle Cross-Section Database for Medical Radioisotope Production: Diagnostic Radioisotopes and Monitor Reactions, IAEA-TECDOC-1211, Vienna, 2001, p. 49 (Chapter 4). Available from: <http://www-nds.indcentre.org.in/reports-new/tecdocs/iaea-tecdoc-1211.pdf>.

[5] S. Takács, F. Szelecsényi, F. Tárkányi, M. Sonck, A. Hermanne, Yu. Shubin, A. Dityuk, M.G. Mustafa, Zhuang Youxiang, New cross-sections and intercomparison of deuteron monitor reactions on Al, Ti, Fe, Ni and Cu, Nucl. Instr. and Meth. B 174 (2001) 235.

[6] G. Székely, FGM – a flexible gamma-spectrum analysis program for a small computer, Comput. Phys. Commun. 34 (1985) 313.

[7] L.P. Ekström, R.B. Firestone, WWW Table of Radioactive Isotopes, Database Version 2/28/99. Available from: <http://ie.lbl.gov/toi/index.htm>.

[8] H.H. Andersen, J.F. Ziegler, The Stopping and Ranges of Ions in Matter, Hydrogen Stopping Powers and Ranges in all Elements, Vol. 3, Pergamon Press, 1977.

[9] Guide to the Expression of Uncertainty in Measurement, International Organization for Standardization, Geneva, 1995, ISBN 92-67-10188-9.

[10] F. Tárkányi, F. Ditrói, J. Csikai, S. Takács, M.S. Uddin, M. Hagiwara, M. Baba, Yu.N. Shubin, A.I. Dityuk, Activation cross-sections of long-lived products of proton-induced nuclear reactions on zinc, Appl. Radiat. Isot. 62 (2005) 73.

[11] A. Hermanne, M. Sonck, S. Takács, F. Tárkányi, Y. Shubin, Study on alternative production of ^{103}Pd and characterisation of contaminants in the deuteron irradiation of ^{103}Rh up to 21 MeV, Nucl. Instr. and Meth. B 187 (2002) 3.

[12] M. Blann, Recent Progress and Current Status of Pre-equilibrium Reaction Theories and Computer Code ALICE, LLNL Report, UCRL-JC-109052, 1991.

[13] A.I. Dityuk, A. Yu. Konobeyev, V.P. Lunev, Yu.N. Shubin, New Advanced Version of Computer Code ALICE–IPPE, Report INDC(CCP)-410, International Atomic Energy Agency, Vienna, 1998.

[14] M. Blann, ALICE-91, Report PSR-0146. Available from: <http://www.nea.fr/abs/html/psr-0146.html>.